Frontiers in Bioscience Landmark

Front. Biosci. (Landmark Ed) **2026**; 31(5): 49658
https://doi.org/10.31083/FBL49658

Original Research

Hypothermic Treatment Alleviates Myocardial Hypertrophy in *bmp10*$^{-/-}$ Zebrafish

Fang Li[1], Ruiqin Hu[1], Beiqi Yang[1], Shouwen Jiang[1], Liangbiao Chen[1,*], Zhong Chen[2,*]

[1]College of Fisheries and Life Science, Shanghai Ocean University, 201306 Shanghai, China
[2]Department of Cardiology, Shanghai Sixth People's Hospital Affiliated to Shanghai Jiao Tong University School of Medicine, 200233 Shanghai, China
*Correspondence: lbchen@shou.edu.cn (Liangbiao Chen); zhongchen7498@hotmail.com (Zhong Chen)
Academic Editor: Natascia Tiso
Submitted: 2 January 2026 Revised: 23 February 2026 Accepted: 9 March 2026 Published: 22 May 2026

Abstract

Background: Cardiac hypertrophy is a major pathological feature of various cardiovascular diseases. Owing to the simple cardiac structure, rapid development, and genetic tractability, zebrafish are an ideal model for studying cardiac pathology. Zebrafish lacking Bone morphogenetic protein 10 (*bmp10*$^{-/-}$) develop myocardial hypertrophy under normothermic conditions (28 °C). However, the long-term effects of chronic cold exposure on cardiac function and survival in this model remain unclear. Therefore, this study utilized the *bmp10*$^{-/-}$ zebrafish model to systematically evaluate the therapeutic potential of chronic hypothermia in attenuating myocardial hypertrophy and to elucidate the underlying molecular mechanisms. **Methods**: This study was conducted in three sequential phases. Phase I: *bmp10*$^{-/-}$ (homozygous mutant, HO) zebrafish at 6 weeks post-fertilization (wpf) were maintained under normothermic (28 °C) or hypothermic (15 °C) conditions for 2 weeks to evaluate the effects of cold exposure on myocardial hypertrophy. Phase II: Building on the Phase I findings, *bmp10*$^{-/-}$ zebrafish were subjected to adaptive temperature-switching between normothermic and hypothermic conditions until 10 wpf to assess the temporal effects of cold exposure on cardiac remodeling. Phase III: Pharmacological validation experiments were performed to identify key regulatory genes mediating hypothermia-induced cardioprotection. **Results**: Long-term cold exposure significantly attenuated myocardial hypertrophy induced by *bmp10* deficiency. Given that hypoxia-inducible factor-1 (HIF-1) is a canonical transcriptional regulator of cellular hypoxic responses and that the stability of HIF-1 is tightly controlled by prolyl hydroxylases such as Egl-9 family hypoxia-inducible factor 3 (EGLN3), the involvement of this pathway was further evaluated. These findings indicate that inhibition of EGLN3 activity stabilizes and activates HIF-1 signaling, thereby mediating cardioprotective effects under hypothermic conditions. **Conclusions**: This study elucidates the functional interplay between the EGLN3 and HIF-1 signaling pathways. Under chronic hypothermia, EGLN3 modulates HIF-1 stability, contributing to the downregulation of BCL2-interacting protein 3 (BNIP3) and facilitating cardiomyocyte injury repair.

Keywords: bone morphogenetic protein 10 (*bmp10*); hypothermia induced; egl-9 family hypoxia-inducible factor 3 (*egln3*); hypoxia-inducible factor-1 (*hif-1*); cardiomegaly

1. Introduction

Cardiac hypertrophy represents an adaptive response of the heart to various physiological and pathological stimuli. Physiological hypertrophy typically occurs in conditions of increased cardiac output demand and is characterized by preserved contractile function and structural integrity. In contrast, pathological hypertrophy—commonly observed in hypertension, myocardial ischemia, and cardiomyopathies—is associated with maladaptive remodeling; including ventricular wall thickening, chamber dilation, and progressive functional deterioration [1–3].

Bone morphogenetic protein 10 (*bmp10*) plays a central role in cardiovascular development and homeostasis [4–6]. It facilitates differentiation of human pluripotent stem cells into cardiovascular progenitors and supports arteriovenous network formation [7–9]. Loss of bmp10 disrupts normal cardiac morphogenesis [10–12], induces anemia and tissue hypoxia [13], and triggers compensatory enhancement of cardiac contractility; thereby exacerbating myocardial hypertrophy [14]. Moreover, *bmp10* deficiency leads to endothelial hyperproliferation and arteriovenous malformations, further impairing oxygen circulation [15,16]. Zebrafish share high conservation with humans in regulatory mechanisms of cardiac development, hypertrophy-related signaling pathways, and embryonic gene reactivation [17–19]. Their genetic manipulability and *in vivo* imaging advantages render them a valuable model for studying cardiac hypertrophy. Recent studies indicate that chronic cold exposure activates multiple protective signaling pathways [20,21], including the hypoxia-inducible factor-1 (*hif-1*) and forkhead box O (*foxo*) pathways; which enhance vascular compliance and reduce oxidative stress and inflammatory responses [22], ultimately decreasing cardiac workload.

Therapeutic hypothermia (TH) is a clinically established intervention that confers protection against ischemia-

reperfusion injury, myocardial infarction, and neurological disorders [23,24]. TH exerts its protective effects by modulating key cellular processes; including hypoxic signaling regulation, apoptosis inhibition, and oxidative stress attenuation [25–28]. Mild hypothermia has been reported to suppress hypoxia-inducible factor-1α (*hif-1*α) activation under ischemic conditions [29–31], thereby influencing downstream pathways involved in angiogenesis and metabolic adaptation. Additionally, TH inhibits mitochondrial-dependent apoptosis by downregulating pro-apoptotic factors such as BCL2 interacting pro- tein 3 (*bnip3*) and BCL2-like 10 (*bcl2l10*), preserving mitochondrial function and limiting reactive oxygen species accumulation. Although previous studies have demonstrated strong similarities between zebrafish and humans in hypertrophy-related signaling and genetic cardiomyopathy phenotypes [32,33], fundamental differences remain in terms of cardiac structure, fibrotic responses, electrophysiological properties, and regenerative capacity; limiting direct translational extrapolation. Against this background, whether cold exposure can modulate hypertrophic phenotypes in genetically modified models such as bmp10 homozygous mutant (*bmp10*$^{-/-}$, HO) zebrafish has not been systematically evaluated.

Therefore, this study focuses on the molecular mechanisms underlying hypothermia-induced reversal of cardiac hypertrophy in *bmp10*-deficient zebrafish, aiming to provide experimental evidence for environmental modulation of myocardial hypertrophy and to expand the investigative scope of the zebrafish model in this field.

2. Materials and Methods

2.1 Generation of bmp10-Deficient Zebrafish

The *bmp10* gene was knocked out in zebrafish using CRISPR–Cas9 technology, generating *bmp10*$^{+/-}$ and *bmp10*$^{-/-}$ mutants. kdrl:EGFP transgenic zebrafish, including *bmp10* wild type (*bmp10*$^{+/+}$, WT) and *bmp10*$^{-/-}$ variants, were derived from the AB wild-type strain (*Danio rerio*), obtained from the National Zebrafish Resource Center (Wuhan, China). These gene-edited zebrafish served as parental fish for generating the *bmp10*$^{-/-}$ offspring. For convenience in selected figure legends, *bmp10*$^{-/-}$ zebrafish are termed HO, and *bmp10*$^{+/+}$ zebrafish as WT. In this study, 15 °C is defined as hypothermic conditions, whereas 28 °C represents normothermic conditions.

The *bmp10* gene is located on chromosome 5. Gene knockout was achieved using the CRISPR–Cas9 system targeting the sequence GGGTTGGATGATGGACATGG, resulting in a 72-bp deletion. gRNA was synthesized using the MAXIscript™ T7 *in vitro* transcription kit (AM1314, Ambion [Invitrogen], Waltham, MA, USA), and Cas9 protein (C120010, Sigma-Aldrich, St. Louis, MO, USA) (800 pg) with gRNA (100 pg) was co-injected into one-cell stage embryos. Genotyping of *bmp10* was performed by PCR using the following primers: forward, ATTTTCATCTGCCACGTCTGC; reverse: TAGAGTTCCAGCATATACTCAG. PCR amplification was conducted using Takara rTaq DNA polymerase (RR901A, Takara Bio Inc., Kusatsu, Shiga, Japan). *bmp10*$^{-/-}$ mutants were identified by agarose gel electrophoresis using molecular biology-grade agarose (75510-019, Invitrogen, Carlsbad, CA, USA).

2.2 Chronic Hypothermic Exposure of Zebrafish

Offspring from *bmp10*$^{+/-}$ self-crosses were raised under normothermic conditions (28 °C) until 6 weeks post fertilization (wpf). Juvenile zebrafish (*bmp10*$^{+/+}$, *bmp10*$^{-/-}$, and *bmp10*$^{+/-}$) were then assigned to either a hypothermic group 15 °C or a normothermic control group 28 °C.

The hypothermic exposure protocol consisted of three stages:

Stage 1: Two-week hypothermic exposure

At 6 wpf, zebrafish were exposed to hypothermic or normothermic conditions for 2 weeks (until 8 wpf; followed by analyses of body weight, cardiac morphology, gene expression, apoptosis, histology, and blood cell counts.

Stage 2: Temperature-switching experiments

(1) Zebrafish exposed to hypothermia from 6–8 wpf were transferred to normothermic conditions until 10 wpf.

(2) Zebrafish maintained under normothermic conditions from 6–8 wpf were transferred to hypothermic conditions until 10 wpf.

Stage 3: Long-term hypothermic exposure

Beginning at 6 wpf, zebrafish were continuously maintained under hypothermic conditions for 8 weeks (until 14 wpf).

2.3 Benazepril Hydrochloride Treatment of bmp10$^{-/-}$ *Zebrafish*

Angiotensin-converting enzyme inhibitors (ACEIs), such as benazepril hydrochloride (HY-B0093A, MedChemExpress, Monmouth Junction, NJ, USA), reduce blood pressure and alleviate cardiac load by inhibiting the renin–angiotensin–aldosterone system. The experiment utilized *bmp10*$^{+/-}$ zebrafish offspring, which were raised at 28 °C until they reached 6 wpf. At the start of the experiment, equal numbers of juveniles (*bmp10*$^{+/+}$; *bmp10*$^{-/-}$) were assigned to either the benazepril hydrochloride treatment group or the control group (which received only the solvent without the drug) for a 2-week treatment period (until 8 wpf). Before the experiment, juveniles in both groups were allocated in equal numbers, with each tank containing no more than 15 juveniles (ensuring a sample size of n $\geq$5 for each group). Benazepril hydrochloride treatment was administered once daily for 1 hour, at a concentration of 50 µM. The working solution was prepared by adding 100 µL of a 25.0 mg/mL dimethyl sulfoxide (DMSO) (HY-Y0320, MedChemExpress, Monmouth Junction, NJ, USA) stock solution to 400 µL of polyethylene glycol 300 (PEG300) (HY-Y0873, MedChemExpress, Monmouth Junction, NJ,

USA), thoroughly mixing. Then, 50 µL of tween-80 (HY-Y1891, MedChemExpress, Monmouth Junction, NJ, USA) was added, followed by mixing, and 450 µL of physiological saline was added to bring the total volume to 1 mL. During the experiment, water quality parameters (including oxygen levels), feeding frequency, and timing were kept consistent between the two groups. Juvenile survival was monitored daily, and a simulated day–night cycle was maintained. At the end of the 2-week treatment (at 8 wpf), the zebrafish from both groups were sampled, and body morphology and cardiac changes in the *bmp10* mutant zebrafish were recorded.

2.4 Cardiac Histological and Histochemical Staining

Zebrafish were anesthetized, and hearts were rapidly dissected and fixed in 4% paraformaldehyde (E672002-0500, BBI Life Sciences, Shanghai, China) at 4 °C for 24 h. Following fixation, samples were subjected to graded ethanol (A500737-0500, BBI Life Sciences, Shanghai, China) dehydration, xylene (X103350, Sinopharm Chemical Reagent Co., Ltd., Beijing, China) clearing, and paraffin embedding. Paraffin-embedded heart tissues were sectioned into 4 µm-thick serial sections using Leica low-profile disposable blades 819 (14035838925, Leica Biosystems, Wetzlar, Germany) for subsequent histological analyses. Heart sections were stained with hematoxylin and eosin staining kit (E607318-0200, BBI Life Sciences, Shanghai, China) and masson's trichrome staining kit (G1340, Solarbio, Beijing, China) in accordance with the manufacturers' instructions to assess overall cardiac morphology and histological features. Images were acquired using a stemi 2000 stereomicroscope (Zeiss, Oberkochen, Germany).

2.5 Confocal Analysis of Myocardial Cell Apoptosis

Myocardial cell apoptosis in cardiac sections (4 µm) was examined using the TUNEL BrightGreen apoptosis detection kit (A112-02, Vazyme Biotech Co, Nanjing, China). The specimens were mounted with anti-fade mounting medium (C02-04003, Bioss Antibodies, Beijing, China) medium for fluorescence and sealed. Apoptotic signals were captured using a LSM710 confocal laser scanning microscope (Carl Zeiss AG, Oberkochen, Germany), and quantitative analysis of the apoptotic signals was performed using ImageJ software (version 1.53, National Institutes of Health, Bethesda, MD, USA).

2.6 Zebrafish Blood Smear Preparation and Staining

Zebrafish were anesthetized with 0.02% tricaine (MS-222) (A5040, Sigma-Aldrich, St. Louis, MO, USA). Approximately 0.5 µL of peripheral blood was collected via tail vein transection and immediately diluted with 2 µL of ultrapure water. The diluted blood was dropped onto one end of a glass slide, and blood smears were prepared using the push–slide method. After air-drying, smears were fixed with absolute methanol (A601617, BBI Life Sciences, Shanghai, China) for 5 min. Blood smears were stained using a Wright–Giemsa staining kit (E607314, BBI Life Sciences, Shanghai, China), and blood cell morphology was analyzed under a light microscope.

2.7 Cardiomyocyte Membrane Staining

Paraffin-embedded zebrafish heart sections were deparaffinized prior to staining. Cell membranes were stained with wheat germ agglutinin, alexa fluor 488 conjugate (G1730, Invitrogen, Carlsbad, CA, USA) for 15 min at room temperature in the dark, followed by three washes with phosphate-buffered saline (PBS) (E607008-0500, BBI Life Sciences, Shanghai, China). Nuclei were counterstained with Hoechst 33258 dye (33258, Solarbio Life Sciences, Beijing, China) for 5 min at room temperature in the dark, followed by PBS washes. After staining, sections were mounted using an anti-fade mounting medium (C02-04003, Bioss Antibodies, Beijing, China) and imaged using a confocal microscope.

2.8 Gene Expression Analysis

Gene sequences for *bmp10*, bone morphogenetic protein 10-like (*bmp10l*), and Hypoxia-inducible factor 3 (*egln3*) were downloaded from the Ensembl website, and primers were designed based on the CDSs of these genes. The primer sequences for *bmp10* were F: ATTTTCATCTGCCACGTCTGC and R: TAGAGTTCCAGCATATACTCAG. The primer sequences for *bmp10l* were F: AGCGGAGATGTACGTGGATT and R: CTGGACGATGGCGTGTTTAG. The primer sequences for *egln3* were F: GCTTTGTTGGATCAGGGCTT and R: GATGTTCCTCCGGCAAACTC. First, RNA extraction was performed using the RNeasy Mini Kit (74104, Qiagen N.V, Hilden, Germany), followed by cDNA synthesis using TransScript Uni All-in-One First-Strand cDNA Synthesis SuperMix for qPCR (AU341-02-V2, TransGen Biotech Co, Beijing, China) with the extracted RNA. Finally, quantitative fluorescence analysis was performed using TB Green Premix Ex Taq II (Tli RNaseH Plus) (RR420A, Takara Bio Inc, Kusatsu, Shiga, Japan) on a CFX Opus 96 Real-Time PCR System (Bio-Rad Laboratories, Inc., Hercules, CA, USA) instrument.

2.9 Statistical Analysis

All statistical analyses were performed using GraphPad Prism software (version 8.0.1, GraphPad Software Inc., San Diego, CA, USA). Data are presented as mean ± standard error of the mean (SEM). Differences between two groups were analyzed using a two-tailed Student's *t*-test. Statistical significance to be defined as $p < 0.05$ (*), $p < 0.01$ (**), $p < 0.001$ (***), and $p < 0.0001$ (****); ns indicates no statistically significant difference.

2.10 Anesthesia and Euthanasia

Zebrafish larvae were immersed in 200 mg/L tricaine (MS-222; Sigma–Aldrich) for approximately 5 minutes until all movement and responses completely ceased. For euthanasia, zebrafish were exposed to an overdose of 400 mg/L tricaine for 15 minutes until they were completely unresponsive and cardiac activity had stopped. To ensure complete death, the fish were subsequently subjected to an ice-water bath at approximately 0 °C for 5 minutes following anesthesia. This procedure was conducted in accordance with the AVMA Guidelines for the Euthanasia of Animals (2020 edition). The tricaine stock was prepared in deionized water and diluted with system water to working concentrations of 200 or 400 mg/L. The pH of the working solutions was adjusted to 7.0–7.5 using sodium bicarbonate ($NaHCO_3$) (A100865-0500, BBI Life Sciences, Shanghai, China).

3. Results

3.1 Chronic Hypothermic Exposure Alleviates Cardiomyocyte Hypertrophy

Chronic hypothermic exposure markedly reversed cardiac hypertrophy in *bmp10*$^{-/-}$ zebrafish (Fig. 1A,B). Under normothermic conditions (28 °C), *bmp10*$^{-/-}$ zebrafish exhibited pronounced cardiac hypertrophy by 8 wpf (Fig. 1A,B). Following chronic hypothermic exposure (15 °C), heart size was reduced in both wild-type and *bmp10*$^{-/-}$ zebrafish, and the difference between the two groups was no longer detectable. These results indicate that hypothermic exposure attenuates myocardial hypertrophy induced by *bmp10* deficiency, rather than producing a mutant-specific effect. Consistently, under normothermic conditions, body weight in 8-week-old *bmp10*$^{-/-}$ zebrafish differed significantly from that of control fish, and this difference was more pronounced than that observed at the early stage (6 weeks of age) (Fig. 1C). Notably, following hypothermic exposure, this difference was markedly abolished (Fig. 1D). Based on these findings, *bmp10*$^{-/-}$ zebrafish were selected as an appropriate experimental model for subsequent mechanistic investigations under hypothermic conditions. Downregulation of *egln3* (Fig. 1G–I) was accompanied by activation of the *hif-1* signaling pathway involved in cardiomyocyte hypoxic responses, together with significant downregulation of the pro-apoptotic genes *bnip3* and *bcl2l10* (Fig. 2F). This molecular profile is consistent with reduced cardiomyocyte size (Fig. 1B) and attenuation of myocardial injury. Although *bmp10l* exhibits partial functional redundancy with *bmp10* during cardiac development, its expression did not fully compensate for the structural defects caused by *bmp10* deficiency (Fig. 1E,F). In addition, hypothermic exposure significantly increased the expression of Kruppel-like factor 1 (*klf1*) in *bmp10*$^{-/-}$ zebrafish hearts (Fig. 2F), a gene implicated in myocardial injury repair and cardiomyocyte proliferation.

3.2 Chronic Hypothermic Exposure Attenuates Myocardial Hypertrophy in *bmp10*$^{-/-}$ Zebrafish by Suppressing Cardiomyocyte Apoptosis

To ameliorate cardiac hypertrophy that had already by 8 wpf, *bmp10*$^{-/-}$ zebrafish were subjected to hypothermic exposure for 2 weeks starting at 6 wpf (Fig. 3Aa). Following hypothermic intervention (15 °C), *bmp10*$^{-/-}$ zebrafish exhibited substantial alterations in overall cardiac morphology (Fig. 2A). Moreover, erythrocyte density within the cardiac chambers showed substantial differences compared with those maintained under normothermic conditions (28 °C) (Fig. 2B). Hypothermic exposure significantly reduced cardiomyocyte apoptosis, as demonstrated by TUNEL staining and quantitative analysis (Fig. 2C,D). Gene expression analysis indicates that *egln3* expression was significantly lower under hypothermic conditions than under normothermic conditions (Fig. 1G–I). These data indicate that *egln3* downregulation may contribute to reduced cardiomyocyte apoptosis in *bmp10*$^{-/-}$ zebrafish.

Forkhead box O (*foxo*) family members (including *foxo3b*, *foxo1a*, and *foxo1b*) can modulate the stability and activity of *hif-1*α by regulating the expression or activity of *egln* genes, thereby influencing cellular responses to hypoxic conditions. The present findings reveal that *foxo*3b increases *hif-1*α activity by suppressing *egln3* expression (Fig. 2F), thereby attenuating the hydroxylation of *hif-1*α. Downregulation of *egln3* through activation of the *hif-1* signaling pathway inhibited excessive apoptosis in *bmp10*$^{-/-}$ cardiac cells, alleviating damage to *bmp10*$^{-/-}$ cardiomyocytes and ultimately protecting cardiac structure and function (Fig. 2E,F). Specifically, reduced *egln3* expression facilitated activation of the anti-apoptotic *hif-1*α signaling pathway, resulting in increased expression of *hif-1*α and its downstream target gene BCL2-like 11 (*bcl2l11*) (Fig. 2F). In parallel, the expression levels of pro-apoptotic genes *bnip3* and *bcl2l10* were correspondingly reduced (Fig. 2F), thereby suppressing mitochondrial outer membrane–mediated apoptotic signaling and attenuating apoptotic signal transmission. Furthermore, exposure to hypothermic conditions increased the expression of uncoupling proteins, including uncoupling protein 1 (*ucp1*) and *ucp3*, in the heart (Fig. 2F); leading to reduced reactive oxygen species production and attenuation of oxidative stress.

3.3 Vascular Development Under Hypothermic Conditions

Fertilized embryos transferred to 15 °C within 3 hours post-fertilization (hpf) resulted in embryonic lethality by 48 hpf. Comparative analysis of cardiac vascular morphology in *bmp10*$^{-/-}$ zebrafish maintained at 28 °C demonstrated substantial differences at 48 and 72 hpf relative to control embryos (Fig. 2G), indicating that *bmp10* plays an essential role in vascular development. Differential gene expression analysis demonstrated significant upregulation of unc-5 netrin receptor b (*unc5b*) and unc-5 netrin receptor da

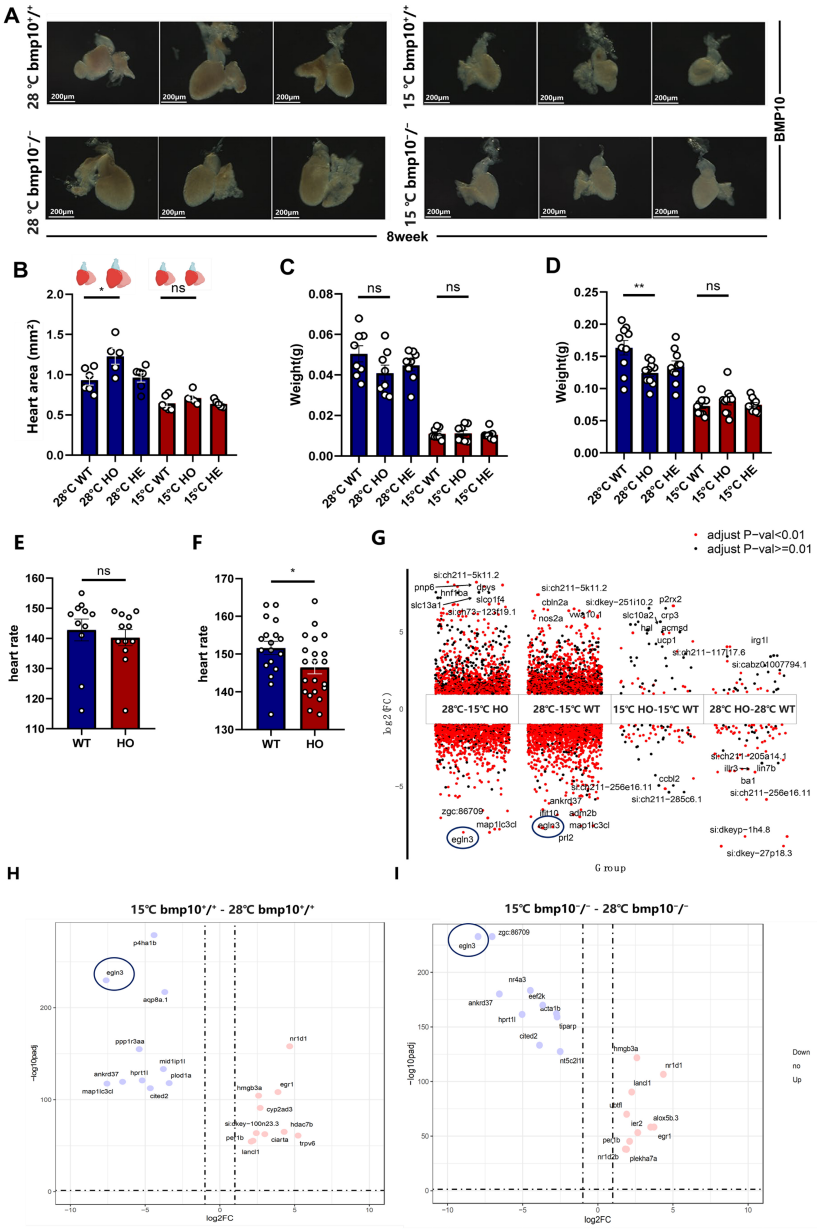

Fig. 1. Comparison of zebrafish lacking bone morphogenetic protein 10 (*bmp10*$^{-/-}$) treated at different temperatures. (A) Calculation of cardiac area based on heart chambers (ventricle, atrium, and bulbus arteriosus). Scale bar = 200 µm. (B) The cardiac area of *bmp10*$^{-/-}$ zebrafish maintained under normothermic conditions (28 °C) was significantly larger than that of *bmp10*$^{-/-}$ zebrafish subjected to chronic cold exposure under hypothermic conditions (15 °C). (C) Body weight of *bmp10*$^{-/-}$ zebrafish at 6 weeks of age (4 weeks of age followed by 2 weeks of hypothermic treatment) under normothermic and hypothermic conditions. (D) Body weight of *bmp10*$^{-/-}$ zebrafish at 8 weeks of age (6 weeks of age followed by 2 weeks of hypothermic treatment) under normothermic and hypothermic conditions. (E) Heart rate measurements of *bmp10*$^{-/-}$ zebrafish at 72–84 hours post-fertilization (hpf) under normothermic conditions (28 °C). (F) Heart rate measurements of *bmp10*$^{-/-}$ zebrafish at 96–108 hpf under normothermic conditions (28 °C). (G) Gene expression comparisons under different temperature conditions: 28 °C–15 °C HO (gene expression differences in *bmp10*$^{-/-}$ zebrafish between 28 °C and 15 °C), 28 °C–15 °C WT (gene expression differences in *bmp10*$^{+/+}$ zebrafish between 28 °C and 15 °C), 15 °C HO–15 °C WT (gene expression differences between *bmp10*$^{-/-}$ and *bmp10*$^{+/+}$ zebrafish at 15 °C), and 28 °C HO–28 °C WT (gene expression differences between *bmp10*$^{-/-}$ and *bmp10*$^{+/+}$ zebrafish at 28 °C). (H) Analysis of Hypoxia-inducible factor-1 (*hif-1*) pathway factor Egl-9 family hypoxia-inducible factor 3 (*egln3*) expression in *bmp10*$^{+/+}$ zebrafish under hypothermic (15 °C) and normothermic (28 °C) conditions. (I) Analysis of *hif-1* pathway factor *egln3* expression in *bmp10*$^{-/-}$ zebrafish under hypothermic (15 °C) and normothermic (28 °C) conditions. Data are presented as mean ± SEM. $p < 0.05$ (*), $p < 0.01$ (**); ns indicates no statistically significant difference.

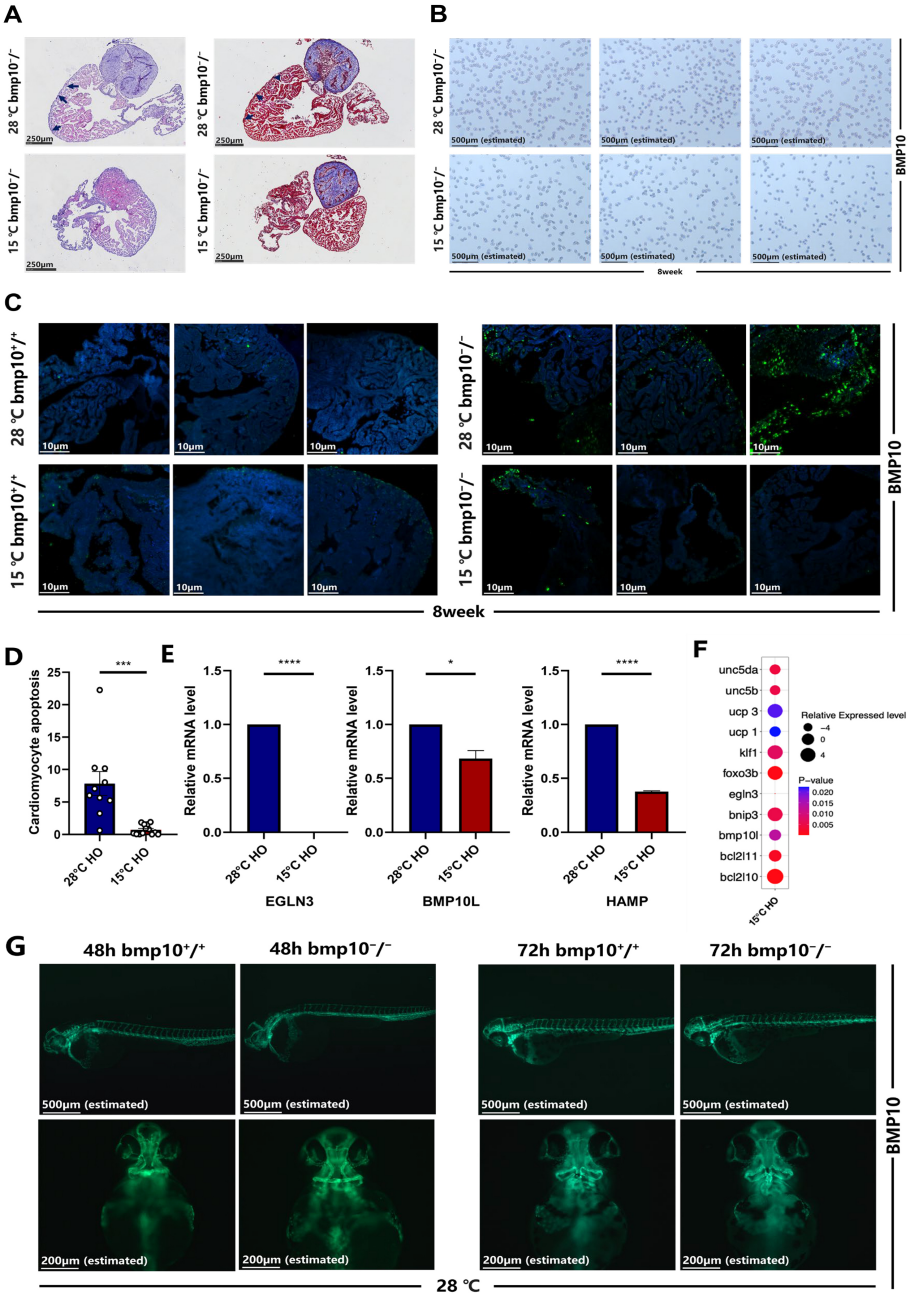

Fig. 2. Chronic cold exposure alleviates cardiomyocyte hypertrophy. (A) Morphological and fibrotic staining analysis of *bmp10*$^{-/-}$ zebrafish hearts after 2 weeks of exposure to hypothermic (15 °C) or normothermic (28 °C) conditions (from 6–8 wpf). Scale bar = 250 μm. (B) Red blood cell density analysis of *bmp10*$^{-/-}$ zebrafish hearts after 2 weeks of exposure to hypothermic (15 °C) or normothermic (28 °C) conditions (from 6–8 wpf). Scale bar = 500 μm (estimated). (C) Cardiomyocyte apoptosis comparison between *bmp10*$^{-/-}$ and *bmp10*$^{+/+}$ zebrafish under different temperature conditions. Scale bar = 10 μm. (D) Quantitative analysis of cardiomyocyte apoptosis in panel C. (E) Relative mRNA expression levels of *egln3*, bone morphogenetic protein 10-like (*bmp10l*), and hepcidin antimicrobial peptide (*hamp*) in *bmp10*$^{-/-}$ zebrafish hearts after 2 weeks of exposure to hypothermic (15 °C) or normothermic (28 °C) conditions (by 8 wpf). (F) Relative mRNA expression levels of *egln3*, Bone morphogenetic protein 10-like (*bmp10l*), Kruppel-like factor 1 (*klf1*), BCL2 interacting protein 3 (*bnip3*), BCL2-like 10 (*bcl2l10*), BCL2-like 11 (*bcl2l11*), forkhead box O (*foxo3b*), Uncoupling protein 1 (*ucp1*), Uncoupling protein 3 (*ucp3*), Unc-5 netrin receptor b (*unc5b*), and Unc-5 netrin receptor da (*unc5da*) in *bmp10*$^{-/-}$ zebrafish cardiomyocytes under hypothermic (15 °C) and normothermic (28 °C) conditions. For individual gene expression levels, refer to **Supplementary Fig. 1**. (G) Imaging of major arteries in *bmp10*$^{-/-}$ and *bmp10*$^{+/+}$ zebrafish at 48 and 72 hpf under normothermic conditions (28 °C). Scale bar = 200 μm (estimated). Data are presented as mean ± SEM. $p < 0.05$ (*), $p < 0.001$ (***), and $p < 0.0001$ (****).

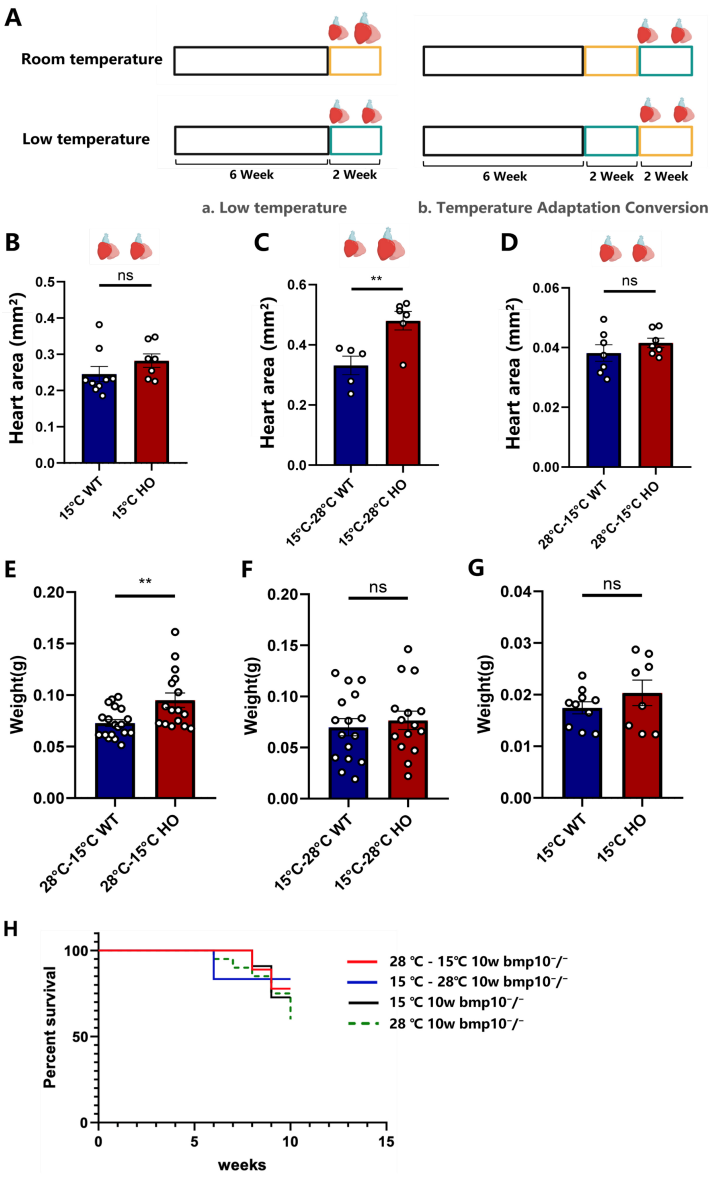

Fig. 3. Cardiac and overall health status of *bmp10*$^{-/-}$ zebrafish following temperature transitions. (A) Low temperature: Normothermic group (Control group)—*bmp10*$^{-/-}$ zebrafish were maintained under normothermic conditions (28 °C) until 8 wpf. Hypothermic group (Experimental group)—*bmp10*$^{-/-}$ zebrafish were maintained under normothermic conditions until 6 wpf and then transferred to hypothermic conditions (15 °C) for 2 weeks (until 8 wpf, green box). Temperature adaptation protocol: (i) *bmp10*$^{-/-}$ zebrafish were maintained under normothermic conditions (28 °C) until 6 wpf, followed by an additional 2 weeks at 28 °C (until 8 wpf; yellow box), and subsequently transferred to hypothermic conditions (15 °C) for 2 weeks (until 10 wpf); (ii) *bmp10*$^{-/-}$ zebrafish were maintained at 28 °C until 6 wpf, then exposed to 15 °C for 2 weeks (green box), and finally returned to 28 °C for an additional 2 weeks (until 10 wpf). (B) Cardiac area comparison between *bmp10*$^{-/-}$ and *bmp10*$^{+/+}$ zebrafish following 8 weeks of chronic cold exposure (until 14 wpf). (C) Cardiac area comparison between *bmp10*$^{-/-}$ and *bmp10*$^{+/+}$ zebrafish after transitioning from hypothermic (15 °C) back to normothermic (28 °C) conditions (until 10 wpf). (D) Cardiac area comparison between *bmp10*$^{-/-}$ and *bmp10*$^{+/+}$ zebrafish after transitioning from normothermic (28 °C) to hypothermic (15 °C) conditions (until 10 wpf). (E) Body weight comparison between *bmp10*$^{-/-}$ and *bmp10*$^{+/+}$ zebrafish following temperature transition from normothermic to hypothermic conditions (until 10 wpf). (F) Body weight comparison between *bmp10*$^{-/-}$ and *bmp10*$^{+/+}$ zebrafish after transitioning from hypothermic back to normothermic conditions (until 10 wpf). (G) Body weight comparison between *bmp10*$^{-/-}$ and *bmp10*$^{+/+}$ zebrafish following 8 weeks of chronic cold exposure (until 14 wpf). (H) Survival rates of *bmp10*$^{-/-}$ zebrafish maintained under normothermic conditions (28 °C) or exposed to three different hypothermic treatment (until 10 wpf). For individual survival curves at each stage, refer to **Supplementary Fig. 2**. Data are presented as mean ± SEM. $p < 0.01$ (**); ns indicates no statistically significant difference.

(*unc5da*) in *bmp10*$^{-/-}$ zebrafish hearts under hypothermic conditions (Fig. 2F). These genes are involved in endothelial cell migration and proliferation and may influence vascular network formation and cardiac contractile function.

3.4 Cardiac Responses to Temperature Transitions

3.4.1 Adaptation to Hypothermic Conditions

bmp10$^{-/-}$ zebrafish exposed to hypothermic conditions (15 °C) for 2 weeks starting at 6 wpf exhibited significant improvement in cardiac hypertrophy (Fig. 1B; Fig. 3Aa). In zebrafish transitioned from normothermic to hypothermic conditions at 8 wpf, morphological abnormalities associated with *bmp10* deficiency were significantly alleviated after 2 weeks of hypothermic exposure (Fig. 3Ab–D; Fig. 3E; Fig. 3F; Fig. 4G,I,J). Survival was also significantly improved compared with zebrafish maintained under normothermic conditions (Fig. 3H).

3.4.2 Hypothermic Preconditioning Followed by Return to Normothermic Conditions

To assess whether the cardioprotective effects of hypothermic exposure were transient, *bmp10*$^{-/-}$ zebrafish were maintained under hypothermic conditions until 8 wpf and then transferred back to normothermic conditions (Fig. 3Ab). The cardioprotective effects persisted following rewarming, with sustained improvements in cardiac morphology and survival (Fig. 3H; Fig. 4H,I,J). Growth delay induced by early-stage hypothermic exposure gradually normalized after return to normothermic conditions (Fig. 3F).

3.5 Hypothermic Exposure Improves Survival of bmp10$^{-/-}$ *Zebrafish*

Under normothermic conditions, *bmp10* deficiency significantly reduced survival after 6 wpf compared with wild-type controls (Fig. 3H). Continuous hypothermic exposure from 6–14 wpf significantly increased survival, reaching 72.7% compared with 45% under normothermic conditions (Fig. 3H). These data demonstrate that chronic hypothermic exposure improves both survival and cardiovascular health in *bmp10*$^{-/-}$ zebrafish (Fig. 4A–F; Fig. 3).

3.6 Angiotensin-converting enzyme inhibitor (ACEI) Mimics the Cardioprotective Effects of Hypothermia

Continuous treatment of *bmp10*$^{-/-}$ zebrafish with benazepril hydrochloride (50 µM, 1 hour daily for two weeks), an ACEI, significantly ameliorated myocardial hypertrophy and reduced cardiomyocyte apoptosis (Fig. 5A–C). Concomitantly, erythrocyte density increased and ventricular wall thickness approached normal levels (Fig. 5D,E). These phenotypic improvements were accompanied by downregulation of *egln3* expression. The molecular and phenotypic alterations induced by ACEI treatment closely resembled those observed under chronic hypothermic exposure (Fig. 5F).

4. Discussion

In this study, the effects of chronic cold exposure on pathological myocardial hypertrophy were systematically evaluated by using the *bmp10*$^{-/-}$ zebrafish model. Sustained hypothermia significantly improved cardiac structural remodeling, reduced cardiomyocyte apoptosis, and enhanced survival. At the molecular level, cold exposure was associated with downregulation of *egln3*, activation of the *hif-1* signaling pathway, and reprogramming of anti-apoptotic gene expression profiles. Together, these changes suggest the establishment of a coordinated adaptive network that mitigates *bmp10* deficiency–induced pathological remodeling.

bmp10 deficiency resulted in progressive ventricular wall thickening and chamber dilation, whereas chronic hypothermia markedly attenuated these structural abnormalities. Morphological and quantitative assessments indicate that cold intervention delayed or partially reversed hypertrophic progression, providing a phenotypic foundation for mechanistic studies. Reduced *egln3* expression under hypothermic conditions coincided with enhanced *hif-1* pathway activity. Given that *egln* family members suppress *hif-1*α stability under normoxic conditions [34–36], hypothermia may alter the hypoxic signaling threshold via modulation of *egln3* expression, thereby facilitating cardiomyocyte adaptive responses. This regulatory process likely represents network-level rebalancing rather than a linear signaling cascade.

In the present model, *egln3* downregulation was accompanied by increased *hif-1* pathway activity, suggesting a functional link between temperature-dependent signaling and hypoxic adaptation in the *bmp10*-deficient heart. *Foxo* family members (including *foxo3b*, *foxo1a*, and *foxo1b*) are participants in hypoxia and stress-responsive signaling networks. The present findings suggest a potential association between *foxo* signaling and *egln3* expression [37–49], possibly contributing to autophagy-related pathways and structural remodeling [50,51]. However, the precise regulatory relationship between *foxo* factors and *egln3* requires further mechanistic investigation. Upregulation of *hif-1*α and its downstream targets was accompanied by downregulation of the pro-apoptotic genes *bnip3* and *bcl2l10* [52,53]. TUNEL and related apoptosis assays confirmed reduced cardiomyocyte apoptosis [54,55]. These results indicate that hypothermia promotes an anti-apoptotic microenvironment and attenuates mitochondrial outer membrane–mediated apoptotic signaling [56]. Furthermore, increased expression of *ucp1* and *ucp3* suggests reduced reactive oxygen species production and alleviation of oxidative stress [57]. Given that oxidative stress is a key driver of hypertrophic progression, hypothermia-induced mitochondrial adaptation may be an important mechanism for preserving cardiac function [58].

Transition from hypothermic to normothermic conditions partially preserved cardioprotective effects. Long-

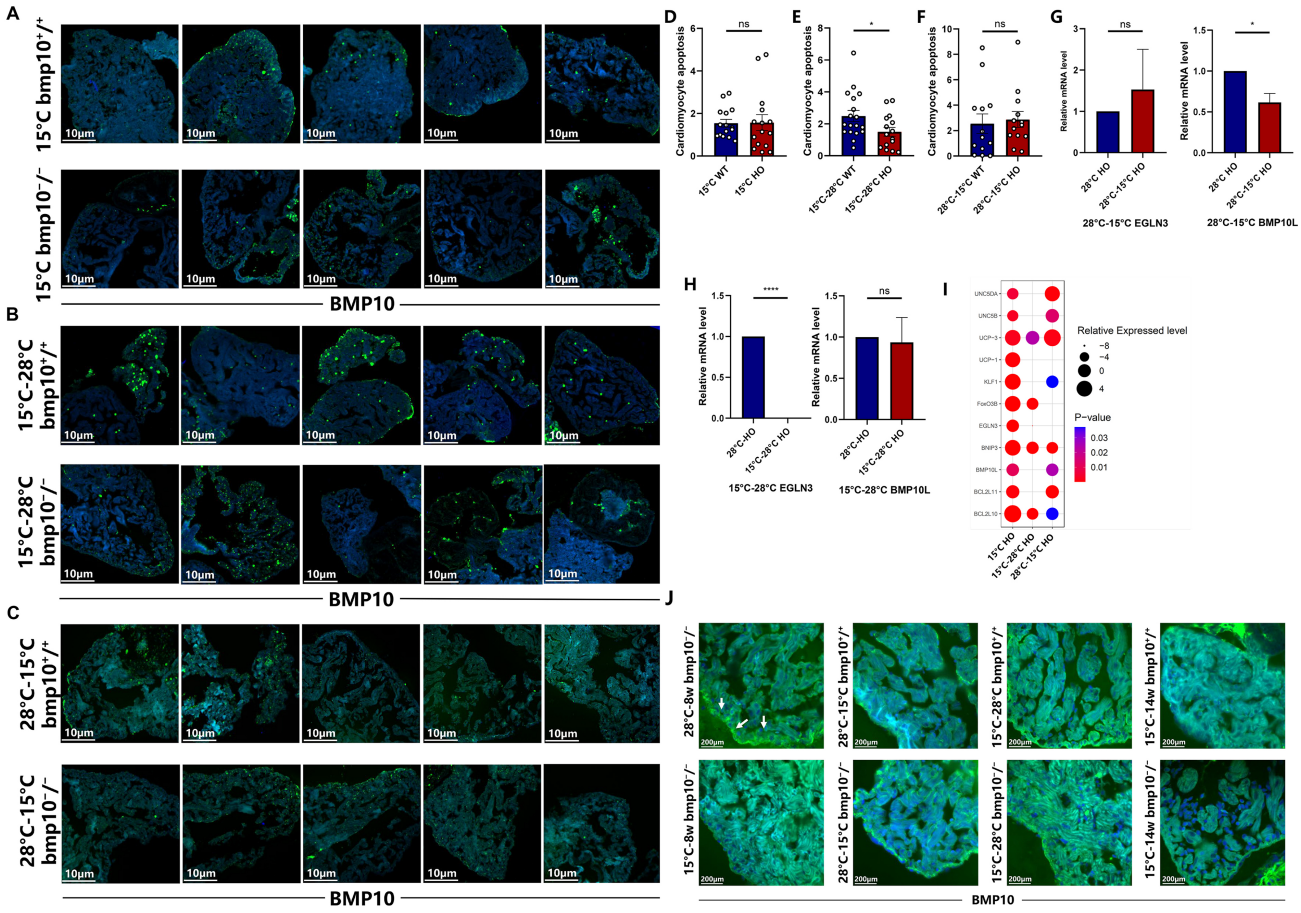

Fig. 4. Sustained improvement in cardiac health following temperature transitions. (A) Cardiomyocyte apoptosis in *bmp10*$^{-/-}$ and *bmp10*$^{+/+}$ zebrafish following 8 weeks of chronic cold exposure (until 14 wpf). Scale bar = 10 μm. (B) Cardiomyocyte apoptosis in *bmp10*$^{-/-}$ and *bmp10*$^{+/+}$ zebrafish after transitioning from hypothermic (15 °C) back to normothermic (28 °C) conditions (until 10 wpf). Scale bar = 10 μm. (C) Cardiomyocyte apoptosis in *bmp10*$^{-/-}$ and *bmp10*$^{+/+}$ zebrafish after transitioning from normothermic (28 °C) to hypothermic (15 °C) conditions (until 10 wpf). Scale bar = 10 μm. (D) Quantitative analysis of cardiomyocyte apoptosis in panel A. (E) Quantitative analysis of cardiomyocyte apoptosis in panel B. (F) Quantitative analysis of cardiomyocyte apoptosis in panel C. (G) Relative expression levels of *egln3* and *bmp10l* after transitioning from normothermic to hypothermic conditions (until 10 wpf). (H) Relative expression levels of *egln3* and *bmp10l* after transitioning from hypothermic back to normothermic conditions (until 10 wpf). (I) Relative expression levels of *egln3*, *bmp10l*, *klf1*, *bnip3*, *bcl2l10*, *bcl2l11*, *foxo3b*, *ucp1*, *ucp3*, *unc5b*, and *unc5da* following three distinct chronic cold exposure paradigms. For individual gene expression data, refer to **Supplementary Figs. 1,3,4**. (J) Morphological analysis of zebrafish cardiomyocytes under different temperature transition paradigms: (i) 2 weeks of cold exposure at 15 °C starting at 6 wpf (until 8 wpf); (ii) 2 weeks at 28 °C followed by 2 weeks at 15 °C (until 10 wpf); (iii) 2 weeks at 15 °C followed by return to 28 °C for 2 weeks (until 10 wpf); and (iv) 8 weeks of chronic cold exposure at 15 °C (until 14 wpf). Scale bar = 200 μm. The area at the edge of the tissue indicated by the white arrow is the ventricular wall of a zebrafish. Data are presented as mean ± SEM. $p < 0.05$ (*), $p < 0.0001$ (****); ns indicates no statistically significant difference.

term hypothermia (6–14 wpf) significantly improved survival [59], with early intervention yielding superior outcomes, underscoring the importance of the therapeutic time window. Pharmacological ACEI treatment partially recapitulated the molecular and phenotypic effects of hypothermia, supporting the involvement of *egln3*-associated signaling networks, although causality remains to be definitively established. Consistent with previous reports, *bmp10* deficiency induces progressive cardiac hypertrophy during early-stage development [60]. As remodeling advances, hypoxia-related signaling, oxidative stress, and cellular stress responses become increasingly pronounced. The present findings suggest that chronic hypothermia modulates these interconnected processes, promoting a more adaptive cardiac phenotype. Whether *bmp10* deficiency results in chamber-specific hypertrophy or regional vulnerability requires further investigation.

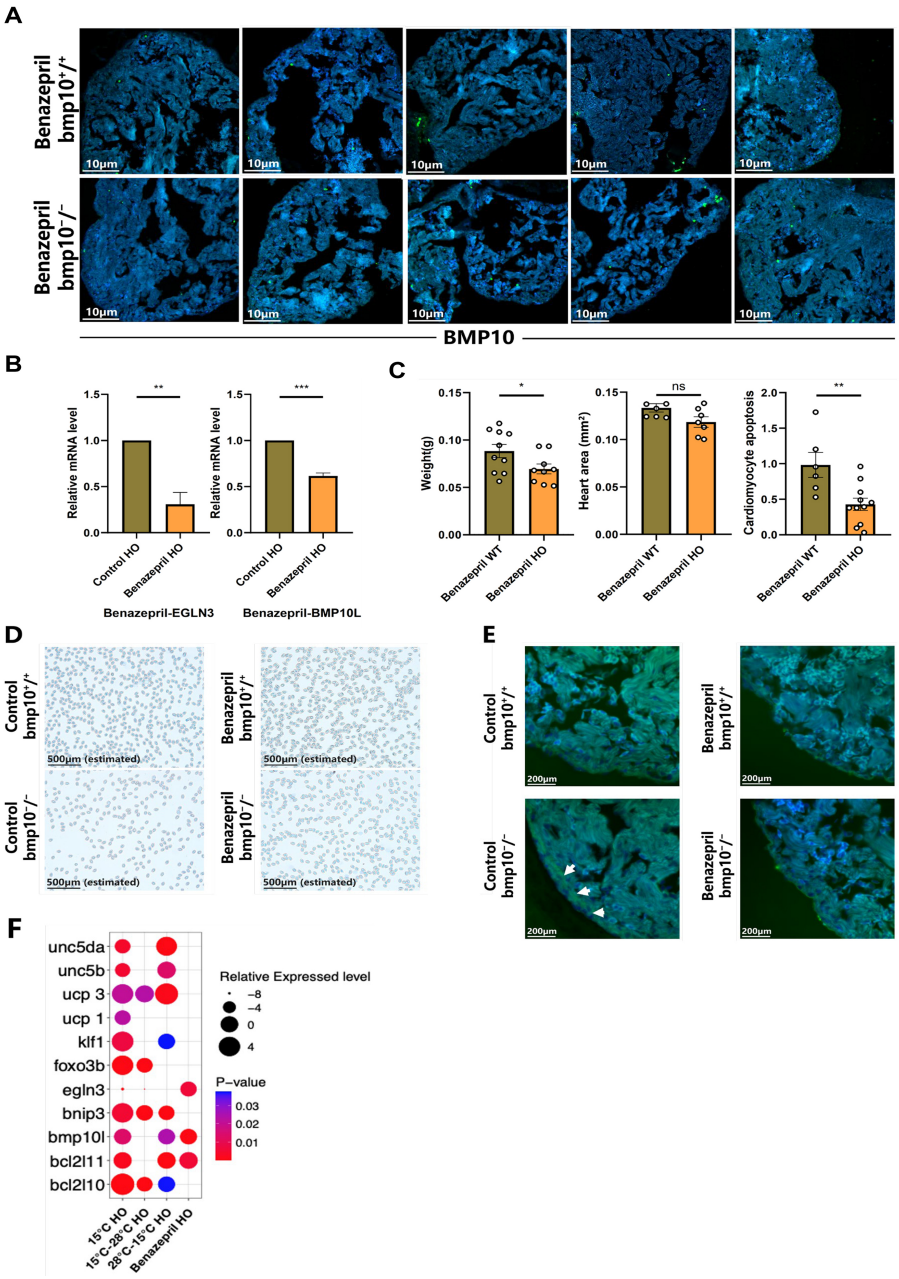

Fig. 5. Treatment of *bmp10*$^{-/-}$ zebrafish with ACEIs. (A) Cardiomyocyte apoptosis in *bmp10*$^{-/-}$ and *bmp10*$^{+/+}$ zebrafish after 2 weeks of ACEI treatment under normothermic conditions (28 °C) (until 10 wpf). Scale bar = 10 μm. (B) Relative expression levels of *egln3* and *bmp10l* following 2 weeks of ACEI treatment (until 10 wpf). (C) Quantitative analysis of body weight, heart area, and cardiomyocyte apoptosis in *bmp10*$^{-/-}$ zebrafish following 2 weeks of ACEI treatment (until 10 wpf). (D) Erythrocyte density in *bmp10*$^{-/-}$ zebrafish following 2 weeks of ACEI treatment (until 10 wpf). Scale bar = 500 μm (estimated). (E) Morphological analysis of myocardial structure in *bmp10*$^{-/-}$ zebrafish following 2 weeks of ACEI treatment (until 10 wpf). Scale bar = 200 μm. The area at the edge of the tissue indicated by the white arrow is the ventricular wall of a zebrafish. (F) Expression levels of *egln3*, *bmp10l*, *klf1*, *bnip3*, *bcl2l10*, *bcl2l11*, *foxo3b*, *ucp1*, *ucp3*, *unc5b*, and *unc5da* following 2 weeks of ACEI treatment. For individual gene expression data, refer to **Supplementary Fig. 5**. Data are presented as mean ± SEM. $p < 0.05$ (*), $p < 0.01$ (**), $p < 0.001$ (***); ns indicates no statistically significant difference.

Collectively, this study identifies hypothermic modulation as a significant environmental determinant of pathological cardiac remodeling. Unlike conventional pharmacological approaches, temperature modulation may exert cardioprotective effects through systemic network reprogramming, offering new insights into adaptive mechanisms under cardiac stress.

5. Limitations

Although the present study demonstrates that chronic hypothermic exposure attenuates myocardial hypertrophy in *bmp10*$^{-/-}$ zebrafish through suppression of cardiomyocyte apoptosis and modulation of the *egln3–hif-1α* signaling axis, several limitations should be acknowledged. First, functional validation of key regulatory components is lacking. Gene-specific loss- or gain-of-function experiments, such as morpholino-mediated knockdown or CRISPR/Cas9-based genetic manipulation of *egln3*, were not performed. Therefore, the necessity and causal contribution of this signaling axis to hypothermia-mediated cardioprotection remain to be definitively established. Second, the current study primarily focuses on transcriptional changes and does not directly assess HIF-1α protein stability or prolyl hydroxylation status under hypothermic conditions. Consequently, the precise post-translational mechanisms through which hypothermia modulates HIF-1 signaling activity require further investigation.

6. Conclusions

In conclusion, using a *bmp10*$^{-/-}$ zebrafish model, this study demonstrates that chronic cold exposure is associated with attenuation of pathological cardiac hypertrophy, reduced cardiomyocyte apoptosis, and improved survival. These beneficial effects coincide with coordinated modulation of hypoxia-related signaling, apoptotic pathways (including *bnip3* and *bcl2l10*), oxidative stress responses (*ucp1* and *ucp3*), and cardiac remodeling markers such as *klf1*. The present findings support the potential relevance of hypothermic modulation in influencing cardiac stress adaptation and pathological remodeling. Rather than establishing a definitive mechanistic pathway, this work provides a data-supported framework suggesting that *egln3*-associated signaling and downstream hypoxia-responsive networks may play important roles in mediating cardioprotective effects under low-temperature conditions. Taken together, this study offers a rationale for further investigation of hypothermia-associated signaling pathways in cardiac disease models. Future studies using mammalian systems and targeted mechanistic approaches will be required to validate these associations and to evaluate the translational potential of hypothermic strategies for chronic cardiac conditions, including hypertrophic cardiomyopathy.

Abbreviations

bmp10, bone morphogenetic protein 10; bmp10l, bone morphogenetic protein 10-like; bmp10$^{-/-}$ (HO), bmp10 homozygous mutant; bmp10$^{+/+}$ (WT), bmp10 wild type; wpf, weeks post fertilization; hpf, hours post-fertilization; egln3, egl-9 family hypoxia-inducible factor 3; hif-1, hypoxia-inducible factor 1; bnip3, BCL2 interacting protein 3; bcl2l10, BCL2-like 10; bcl2l11, BCL2-like 11; foxo, forkhead box O; ucp1, uncoupling protein 1; ucp3, uncoupling protein 3; unc5b, Unc-5 netrin receptor B; unc5da, Unc-5 netrin receptor da; ACE, angiotensin-converting enzyme; ACEI, angiotensin-converting enzyme inhibitor; TH, therapeutic hypothermia.

Availability of Data and Materials

Further information and requests should be directed to the lead contact, Ph.D, Professor Zhong Chen (zhongchen7498@hotmail.com).

Author Contributions

FL, ZC, and LBC designed the study and contributed to the conceptualization of the manuscript. FL drafted the original manuscript and contributed to writing, editing, visualization, validation, software, resources, methodology, investigation, and data management. ZC and LBC reviewed and edited the manuscript, and contributed to methodology, supervision, validation, resources, investigation, formal analysis, and funding acquisition. RQH participated in manuscript review and editing, and contributed to resources, investigation, formal analysis, supervision, validation, data acquisition, and analysis. BQY contributed to manuscript review and editing, visualization, software, validation, data acquisition and analysis, and supervision. SWJ participated in manuscript review and editing, provided resources, and contributed to formal analysis, data acquisition and analysis, investigation, validation, and supervision. All authors contributed to manuscript revision and editing, have read and approved the final version, and agree to be accountable for all aspects of the work.

Ethics Approval and Consent to Participate

All animal experiments were conducted in accordance with the institutional guidelines of Shanghai Ocean University and complied with the European Union Directive 2010/63/EU on the protection of animals used for scientific purposes, as well as the ARRIVE 2.0 guidelines. The experimental protocol was reviewed and approved by the Animal Welfare and Ethical Review Body (AWERB) of Shanghai Ocean University (Approval No. SHOU-DW-2021-068). Ethical assessment of animal use was performed in accordance with Directive 2010/63/EU, which provides a regulatory framework for ethical review and risk assessment in scientific research involving animals. The study strictly adhered to the principles of Replacement, Reduction, and Refinement (3R). Experimental necessity was carefully evaluated during study design, procedures were optimized, and appropriate measures were implemented to minimize animal numbers as well as potential pain and distress.

Acknowledgment

The authors thank all individuals who contributed to the preparation of this manuscript. The authors also appreciate the constructive comments and valuable sugges-

tions provided by the peer reviewers, which substantially improved the quality and clarity of this work.

Funding

This study was funded by National Natural Science Foundation of China Key Project (32130109) and Funds of Shanghai Sixth People's Hospital (2017006).

Conflict of Interest

The authors declare no conflict of interest.

Supplementary Material

Please refer to the supplementary materials (S1, S2, S3, S4, S5) for additional information. Supplementary material associated with this article can be found, in the online version, at https://doi.org/10.31083/FBL49658.

References

[1] Wang L, Rice M, Swist S, Kubin T, Wu F, Wang S, *et al*. BMP9 and BMP10 Act Directly on Vascular Smooth Muscle Cells for Generation and Maintenance of the Contractile State. Circulation. 2021; 143: 1394–1410. https://doi.org/10.1161/CIRCULATIONAHA.120.047375.

[2] Chen H, Brady Ridgway J, Sai T, Lai J, Warming S, Chen H, *et al*. Context-dependent signaling defines roles of BMP9 and BMP10 in embryonic and postnatal development. Proceedings of the National Academy of Sciences of the United States of America. 2013; 110: 11887–11892. https://doi.org/10.1073/pnas.1306074110.

[3] Ommen SR, Mital S, Burke MA, Day SM, Deswal A, Elliott P, *et al*. 2020 AHA/ACC Guideline for the Diagnosis and Treatment of Patients With Hypertrophic Cardiomyopathy: A Report of the American College of Cardiology/American Heart Association Joint Committee on Clinical Practice Guidelines. Journal of the American College of Cardiology. 2020; 76: e159–e240. https://doi.org/10.1016/j.jacc.2020.08.045.

[4] Zhang W, Chen H, Wang Y, Yong W, Zhu W, Liu Y, *et al*. Tbx20 transcription factor is a downstream mediator for bone morphogenetic protein-10 in regulating cardiac ventricular wall development and function. The Journal of Biological Chemistry. 2011; 286: 36820–36829. https://doi.org/10.1074/jbc.M111.279679.

[5] Chen H, Yong W, Ren S, Shen W, He Y, Cox KA, *et al*. Overexpression of bone morphogenetic protein 10 in myocardium disrupts cardiac postnatal hypertrophic growth. The Journal of Biological Chemistry. 2006; 281: 27481–27491. https://doi.org/10.1074/jbc.M604818200.

[6] Pashmforoush M, Lu JT, Chen H, Amand TS, Kondo R, Pradervand S, *et al*. Nkx2-5 pathways and congenital heart disease; loss of ventricular myocyte lineage specification leads to progressive cardiomyopathy and complete heart block. Cell. 2004; 117: 373–386. https://doi.org/10.1016/s0092-8674(04)00405-2.

[7] Mikryukov AA, Mazine A, Wei B, Yang D, Miao Y, Gu M, *et al*. BMP10 Signaling Promotes the Development of Endocardial Cells from Human Pluripotent Stem Cell-Derived Cardiovascular Progenitors. Cell Stem Cell. 2021; 28: 96–111.e7. https://doi.org/10.1016/j.stem.2020.10.003.

[8] Chen H, Shi S, Acosta L, Li W, Lu J, Bao S, et al. BMP10 is essential for maintaining cardiac growth during murine cardiogenesis. Development (Cambridge, England). 2004; 131: 2219–2231. https://doi.org/10.1242/dev.01094.

[9] Choi H, Kim BG, Kim YH, Lee SJ, Lee YJ, Oh SP. BMP10 functions independently from BMP9 for the development of a proper arteriovenous network. Angiogenesis. 2023; 26: 167–186. https://doi.org/10.1007/s10456-022-09859-0.

[10] Capasso TL, Li B, Volek HJ, Khalid W, Rochon ER, Anbalagan A, *et al*. BMP10-mediated ALK1 signaling is continuously required for vascular development and maintenance. Angiogenesis. 2020; 23: 203–220. https://doi.org/10.1007/s10456-019-09701-0.

[11] Leggit JC, Whitaker D. Diagnosis and Management of Hypertrophic Cardiomyopathy: Updated Guidelines From the ACC/AHA. American Family Physician. 2022; 105: 207–209.

[12] Maron BJ, Maron MS. Hypertrophic cardiomyopathy. Lancet (London, England). 2013; 381: 242–255. https://doi.org/10.1016/S0140-6736(12)60397-3.

[13] Hu R, Li G, Hu P, Niu H, Li W, Jiang S, *et al*. bmp10 maintains cardiac function by regulating iron homeostasis. Journal of Genetics and Genomics = Yi Chuan Xue Bao. 2024; 51: 1459–1473. https://doi.org/10.1016/j.jgg.2024.10.003.

[14] Grego-Bessa J, Luna-Zurita L, del Monte G, Bolós V, Melgar P, Arandilla A, *et al*. Notch signaling is essential for ventricular chamber development. Developmental Cell. 2007; 12: 415–429. https://doi.org/10.1016/j.devcel.2006.12.011.

[15] Neuhaus H, Rosen V, Thies RS. Heart specific expression of mouse BMP-10 a novel member of the TGF-beta superfamily. Mechanisms of Development. 1999; 80: 181–184. https://doi.org/10.1016/s0925-4773(98)00221-4.

[16] Reyat JS, Chua W, Cardoso VR, Witten A, Kastner PM, Kabir SN, *et al*. Reduced left atrial cardiomyocyte PITX2 and elevated circulating BMP10 predict atrial fibrillation after ablation. JCI Insight. 2020; 5: e139179. https://doi.org/10.1172/jci.insight.139179.

[17] Narumanchi S, Wang H, Perttunen S, Tikkanen I, Lakkisto P, Paavola J. Zebrafish Heart Failure Models. Frontiers in Cell and Developmental Biology. 2021; 9: 662583. https://doi.org/10.3389/fcell.2021.662583.

[18] Romano N, Ceci M. Are microRNAs responsible for cardiac hypertrophy in fish and mammals? What we can learn in the activation process in a zebrafish ex vivo model. Biochimica et Biophysica Acta. Molecular Basis of Disease. 2020; 1866: 165896. https://doi.org/10.1016/j.bbadis.2020.165896.

[19] Ceci M, Bonvissuto D, Papetti F, Silvestri F, Sette C, Catalani E, *et al*. RACK1 contributes to the upregulation of embryonic genes in a model of cardiac hypertrophy. Scientific Reports. 2024; 14: 25698. https://doi.org/10.1038/s41598-024-76138-x.

[20] Jurado-Fasoli L, Sanchez-Delgado G, Di X, Yang W, Kohler I, Villarroya F, *et al*. Cold-induced changes in plasma signaling lipids are associated with a healthier cardiometabolic profile independently of brown adipose tissue. Cell Reports. Medicine. 2024; 5: 101387. https://doi.org/10.1016/j.xcrm.2023.101387.

[21] Hanssen MJW, Hoeks J, Brans B, van der Lans AAJJ, Schaart G, van den Driessche JJ, *et al*. Short-term cold acclimation improves insulin sensitivity in patients with type 2 diabetes mellitus. Nature Medicine. 2015; 21: 863–865. https://doi.org/10.1038/nm.3891.

[22] Li X, Wu F, Günther S, Looso M, Kuenne C, Zhang T, *et al*. Inhibition of fatty acid oxidation enables heart regeneration in adult mice. Nature. 2023; 622: 619–626. https://doi.org/10.1038/s41586-023-06585-5.

[23] Shi J, Dai W, Kloner RA. Therapeutic Hypothermia Reduces the Inflammatory Response Following Ischemia/Reperfusion Injury in Rat Hearts. Therapeutic Hypothermia and Temperature Management. 2017; 7: 162–170. https://doi.org/10.1089/ther.2016.0042.

[24] Hong JM, Lee JS, Song HJ, Jeong HS, Choi HA, Lee K. Therapeutic hypothermia after recanalization in patients with acute

ischemic stroke. Stroke. 2014; 45: 134–140. https://doi.org/10.1161/STROKEAHA.113.003143.

[25] Morrell NW, Bloch DB, ten Dijke P, Goumans MJTH, Hata A, Smith J, *et al*. Targeting BMP signalling in cardiovascular disease and anaemia. Nature Reviews. Cardiology. 2016; 13: 106–120. https://doi.org/10.1038/nrcardio.2015.156.

[26] Dong BB, Li YJ, Liu XY, Huang RT, Yang CX, Xu YJ, *et al*. Discovery of *BMP10* as a new gene underpinning congenital heart defects. American Journal of Translational Research. 2024; 16: 109–125. https://doi.org/10.62347/IVRF4475.

[27] Tanaka K, Honda M, Takabatake T. Redox regulation of MAPK pathways and cardiac hypertrophy in adult rat cardiac myocyte. Journal of the American College of Cardiology. 2001; 37: 676–685. https://doi.org/10.1016/s0735-1097(00)01123-2.

[28] Hilfiker-Kleiner D, Shukla P, Klein G, Schaefer A, Stapel B, Hoch M, *et al*. Continuous glycoprotein-130-mediated signal transducer and activator of transcription-3 activation promotes inflammation, left ventricular rupture, and adverse outcome in subacute myocardial infarction. Circulation. 2010; 122: 145–155. https://doi.org/10.1161/CIRCULATIONAHA.109.933127.

[29] Willam C, Maxwell PH, Nichols L, Lygate C, Tian YM, Bernhardt W, *et al*. HIF prolyl hydroxylases in the rat; organ distribution and changes in expression following hypoxia and coronary artery ligation. Journal of Molecular and Cellular Cardiology. 2006; 41: 68–77. https://doi.org/10.1016/j.yjmcc.2006.04.009.

[30] Pescador N, Cuevas Y, Naranjo S, Alcaide M, Villar D, Landázuri MO, *et al*. Identification of a functional hypoxia-responsive element that regulates the expression of the egl nine homologue 3 (egln3/phd3) gene. The Biochemical Journal. 2005; 390: 189–197. https://doi.org/10.1042/BJ20042121.

[31] Jin Y, Pan Y, Zheng S, Liu Y, Xu J, Peng Y, *et al*. Inactivation of EGLN3 hydroxylase facilitates Erk3 degradation via autophagy and impedes lung cancer growth. Oncogene. 2022; 41: 1752–1766. https://doi.org/10.1038/s41388-022-02203-2.

[32] Yang T, Zhang Z, Huang S, Cui M, Liu S, Ding M, *et al*. Construction of a Zebrafish Model of Cardiac Hypertrophy Caused by ATIC Gene Deletion and Preliminary Exploration of Aerobic Exercise Improvement. International Journal of Molecular Sciences. 2025; 26: 10249. https://doi.org/10.3390/ijms262110249.

[33] Huang L, Gao D, Zhang Y, Wang C, Zuo Z. Exposure to low dose benzo [a] pyrene during early life stages causes symptoms similar to cardiac hypertrophy in adult zebrafish. Journal of hazardous materials. 2014; 276: 377–382. https://doi.org/10.1016/j.jhazmat.2014.05.057

[34] Fu J, Menzies K, Freeman RS, Taubman MB. EGLN3 prolyl hydroxylase regulates skeletal muscle differentiation and myogenin protein stability. The Journal of Biological Chemistry. 2007; 282: 12410–12418. https://doi.org/10.1074/jbc.M608748200.

[35] Schödel J, Ratcliffe PJ. Mechanisms of hypoxia signalling: new implications for nephrology. Nature Reviews. Nephrology. 2019; 15: 641–659. https://doi.org/10.1038/s41581-019-0182-z.

[36] Yuan X, Ruan W, Bobrow B, Carmeliet P, Eltzschig HK. Targeting hypoxia-inducible factors: therapeutic opportunities and challenges. Nature Reviews. Drug Discovery. 2024; 23: 175–200. https://doi.org/10.1038/s41573-023-00848-6.

[37] Kong X, Liu H, He X, Sun Y, Ge W. Unraveling the Mystery of Cold Stress-Induced Myocardial Injury. Frontiers in Physiology. 2020; 11: 580811. https://doi.org/10.3389/fphys.2020.580811.

[38] Sluse FE, Jarmuszkiewicz W, Navet R, Douette P, Mathy G, Sluse-Goffart CM. Mitochondrial UCPs: new insights into regulation and impact. Biochimica et Biophysica Acta. 2006; 1757: 480–485. https://doi.org/10.1016/j.bbabio.2006.02.004.

[39] Yenari MA, Hemmen TM. Therapeutic hypothermia for brain ischemia: where have we come and where do we go? Stroke. 2010; 41: S72–S74. https://doi.org/10.1161/STROKEAHA.110.595371.

[40] Zhao MT, Ye S, Su J, Garg V. Cardiomyocyte Proliferation and Maturation: Two Sides of the Same Coin for Heart Regeneration. Frontiers in Cell and Developmental Biology. 2020; 8: 594226. https://doi.org/10.3389/fcell.2020.594226.

[41] Liu Y, Chen X, Zhang HG. Editorial: Cardiac Hypertrophy: From Compensation to Decompensation and Pharmacological Interventions. Frontiers in Pharmacology. 2021; 12: 665936. https://doi.org/10.3389/fphar.2021.665936.

[42] Dansen TB, Burgering BMT. Unravelling the tumor-suppressive functions of FOXO proteins. Trends in Cell Biology. 2008; 18: 421–429. https://doi.org/10.1016/j.tcb.2008.07.004.

[43] van der Vos KE, Coffer PJ. FOXO-binding partners: it takes two to tango. Oncogene. 2008; 27: 2289–2299. https://doi.org/10.1038/onc.2008.22.

[44] Calnan DR, Brunet A. The FoxO code. Oncogene. 2008; 27: 2276–2288. https://doi.org/10.1038/onc.2008.21.

[45] Gross DN, van den Heuvel APJ, Birnbaum MJ. The role of FoxO in the regulation of metabolism. Oncogene. 2008; 27: 2320–2336. https://doi.org/10.1038/onc.2008.25.

[46] Strocchi S, Reggiani F, Gobbi G, Ciarrocchi A, Sancisi V. The multifaceted role of EGLN family prolyl hydroxylases in cancer: going beyond HIF regulation. Oncogene. 2022; 41: 3665–3679. https://doi.org/10.1038/s41388-022-02378-8.

[47] Martins R, Lithgow GJ, Link W. Long live FOXO: unraveling the role of FOXO proteins in aging and longevity. Aging Cell. 2016; 15: 196–207. https://doi.org/10.1111/acel.12427.

[48] Polytarchou C, Iliopoulos D, Hatziapostolou M, Kottakis F, Maroulakou I, Struhl K, *et al*. Akt2 regulates all Akt isoforms and promotes resistance to hypoxia through induction of miR-21 upon oxygen deprivation. Cancer Research. 2011; 71: 4720–4731. https://doi.org/10.1158/0008-5472.CAN-11-0365.

[49] Li L, Kang H, Zhang Q, D'Agati VD, Al-Awqati Q, Lin F. FoxO3 activation in hypoxic tubules prevents chronic kidney disease. The Journal of Clinical Investigation. 2019; 129: 2374–2389. https://doi.org/10.1172/JCI122256.

[50] Nguyen PD, Gooijers I, Campostrini G, Verkerk AO, Honkoop H, Bouwman M, *et al*. Interplay between calcium and sarcomeres directs cardiomyocyte maturation during regeneration. Science (New York, N.Y.). 2023; 380: 758–764. https://doi.org/10.1126/science.abo6718.

[51] Da'as SI, Hasan W, Salem R, Younes N, Abdelrahman D, Mohamed IA, *et al*. Transcriptome Profile Identifies Actin as an Essential Regulator of Cardiac Myosin Binding Protein C3 Hypertrophic Cardiomyopathy in a Zebrafish Model. International Journal of Molecular Sciences. 2022; 23: 8840. https://doi.org/10.3390/ijms23168840.

[52] Zhang J, Ney PA. Role of BNIP3 and NIX in cell death, autophagy, and mitophagy. Cell Death and Differentiation. 2009; 16: 939–946. https://doi.org/10.1038/cdd.2009.16.

[53] Hamacher-Brady A, Brady NR, Logue SE, Sayen MR, Jinno M, Kirshenbaum LA, *et al*. Response to myocardial ischemia/reperfusion injury involves Bnip3 and autophagy. Cell Death and Differentiation. 2007; 14: 146–157. https://doi.org/10.1038/sj.cdd.4401936.

[54] Guo K, Searfoss G, Krolikowski D, Pagnoni M, Franks C, Clark K, *et al*. Hypoxia induces the expression of the pro-apoptotic gene BNIP3. Cell Death and Differentiation. 2001; 8: 367–376. https://doi.org/10.1038/sj.cdd.4400810.

[55] González A, Fortuño MA, Querejeta R, Ravassa S, López B, López N, *et al*. Cardiomyocyte apoptosis in hypertensive cardiomyopathy. Cardiovascular Research. 2003; 59: 549–562. https://doi.org/10.1016/s0008-6363(03)00498-x.

[56] Rikka S, Quinsay MN, Thomas RL, Kubli DA, Zhang X, Murphy AN, *et al*. Bnip3 impairs mitochondrial bioenergetics and stimulates mitochondrial turnover. Cell Death and Differentiation. 2011; 18: 721–731. https://doi.org/10.1038/cdd.2010.146.

[57] Bouillaud F, Alves-Guerra MC, Ricquier D. UCPs, at the interface between bioenergetics and metabolism. Biochimica et Biophysica Acta. 2016; 1863: 2443–2456. https://doi.org/10.1016/j.bbamcr.2016.04.013.

[58] Ehata S, Miyazono K. Bone Morphogenetic Protein Signaling in Cancer; Some Topics in the Recent 10 Years. Frontiers in Cell and Developmental Biology. 2022; 10: 883523. https://doi.org/10.3389/fcell.2022.883523.

[59] Seki T, Yang Y, Sun X, Lim S, Xie S, Guo Z, *et al*. Brown-fat-mediated tumour suppression by cold-altered global metabolism. Nature. 2022; 608: 421–428. https://doi.org/10.1038/s41586-022-05030-3.

[60] Bouvard C, Tu L, Rossi M, Desroches-Castan A, Berrebeh N, Helfer E, *et al*. Different cardiovascular and pulmonary phenotypes for single- and double-knock-out mice deficient in BMP9 and BMP10. Cardiovascular Research. 2022; 118: 1805–1820. https://doi.org/10.1093/cvr/cvab187.